

The Comparison of Stellar Atmospheric Parameters between LAMOST and APOGEE databases

Y.Q. Chen¹, G. Zhao¹, C. Liu¹, J. Ren¹, Y.P. Jia¹, J.K. Zhao¹, A.L. Luo¹, Y. Zhang², Y.H. Hou², Y.F. Wang² & M. Yang²

¹ Key Laboratory of Optical Astronomy, National Astronomical Observatories, Chinese Academy of Sciences, Beijing, 100012, China; cyq@bao.ac.cn

² Nanjing Institute of Astronomical Optics & Technology, National Astronomical Observatories, Chinese Academy of Sciences, Nanjing 210042, China

Abstract We have compared the stellar parameters, temperature, gravity and metallicity, between the LAMOST-DR2 and SDSS-DR12/APOGEE database for stars in common. It is found that the LAMOST database provides a better red-clump feature than the APOGEE database in the T_{eff} versus $\log g$ diagram. With this advantage, we have separated red clump stars from red giant stars, and attempt to establish the calibrations between the two datasets for the two groups of stars respectively.

It shows that there is a good consistency in temperature with a calibration close to the one-to-one line, and we can establish a satisfied metallicity calibration of $[Fe/H]_{APOGEE} = 1.18[Fe/H]_{LAMOST} + 0.11$ with a scatter of ~ 0.08 dex for both red clump and red giant branch samples. For gravity, there is no any correlation for red clump stars between the two databases, and scatters around the calibrations of red giant stars are substantial. We found two main sources of the scatters of $\log g$ for red giant stars. One is a group of stars with $0.00253 * T_{eff} - 8.67 < \log g < 2.6$ locating at the forbidden region, and the other is the contaminated red clump stars, which could be picked out from the unmatched region where stellar metallicity is not consistent with the position in the T_{eff} versus $\log g$ diagram. After excluding stars at the two regions, we have established two calibrations for red giant stars, $\log g_{APOGEE} = 0.000615 * T_{eff_{LAMOST}} + 0.697 * \log g_{LAMOST} - 2.208$ ($\sigma = 0.150$) for $[Fe/H] > -1$ and $\log g_{APOGEE} = 0.000874 * T_{eff_{LAMOST}} + 0.588 * \log g_{LAMOST} - 3.117$ ($\sigma = 0.167$) for $[Fe/H] < -1$. The calibrations are valid for stars with $T_{eff} = 3800 - 5400$ K and $\log g = 0 - 3.8$ dex, and are useful in a work aiming to combine the LAMOST and APOGEE databases in the future study. In addition, we find that an SVM method based on seismic $\log g$ is a good way to greatly improve the accuracy of gravity for these two regions at least in the LAMOST database.

Key words: stars: late type – stars: fundamental parameters – stars: atmospheres – stars: abundances

1 INTRODUCTION

Stellar spectroscopic survey provides an important source of knowledge in astrophysics. The information from spectroscopy include physical parameters of stars (temperatures, gravities and detailed chemical composition) and their kinematics (radial velocities), which are crucial to our understanding of stars and stellar populations in the Milky Way and other galaxies. The advent of large stellar spectroscopic surveys like SEGUE/SDSS (Yanny et al. 2009), RAVE (Kordopatis et al. 2013), APOGEE (Majewski

et al. 2015), and the LAMOST (Zhao et al. 2012) is leading Galactic astronomy into a precision science, where we can identify different sub-populations by combining the chemical composition with kinematics and trace Galactic evolution and stellar structure at various Galactic locations in details.

Recently, the LAMOST telescope, also known as the Wang-Su Reflecting Schmidt Telescope or the Guoshoujing Telescope (Cui et al. 2012), has finished a two year regular survey after one year's pilot survey in 2011. The combination of a large aperture (4 m) and high multiplex factor (4000 fibers) with a 5 degree field of view makes it a unique facility. With the low-resolution ($R = 1800$), the LAMOST project currently presents spectra of $\sim 4,136,000$ objects and stellar parameters for $\sim 2,200,000$ stars in its second data release (Luo et al. 2015). This database includes many previously observed Kepler targets provided by the LAMOST-Kepler project (Cat et al. 2014). More detailed information on the data release can be found in the website (<http://www.lamost.org/public/>). Stellar parameters in the LAMOST DR2 database are derived by the package *ULySS* (Wu et al. 2011), where an observed spectrum is fitted against a model expressed as a linear combination of non-linear components, optionally convolved with a line-of-sight velocity distribution (LOSVD) and multiplied with a polynomial function.

Coincidentally, APOGEE (Majewski et al. 2015) has released its three-year, near-infrared survey for 100,000 red giant stars included as part of the SDSS-III (Eisenstein et al. 2011; Ahn et al. 2012). With a resolving power of 22,500, APOGEE is able to derive detailed abundances for 15 elements as well as the three basic stellar parameters, temperatures, gravities and metallicities. Based on a synthetic grid of Kurucz models and an efficient search method, a best match within the synthetic grid is found for each APOGEE spectrum to provide the initial set of parameters: T_{eff} , $\log g$, $[M/H]$, $[C/M]$, $[N/M]$, and $[\alpha/M]$. Then the stellar parameters are calibrated by giants in the Kepler field and stars in the clusters.

The main population of the observed targets in both the LAMOST and APOGEE surveys is the Galactic disk. In principle, they can be merged together to probe the property of the Galactic disk, and the results obtained from either one can be checked in an independent way. Meanwhile, the two surveys are quite different in many ways. They have different observed bands, resolving powers of the spectra, and thus they can provide abundances for different elements and kinematics with different precisions. The two surveys have their own advantages in the sky coverage, selection function and stellar spectral type. Thus, it is important to mix these information together in order to understand the history of the Galactic disk from different views as well as checking if the results from either survey are reliable or not. In view of this, we aim to make a systematical study on the chemical and kinematic properties of the Galactic disk by combining the data from the two surveys in the near future. This combination is particularly important for the study of the local effect of the chemical evolution, stellar migration of the Galactic disk and the understanding of the origins of many kinematical structures in the Galactic disk.

It is interesting to know how consistent stellar parameters between the LAMOST and APOGEE databases are, and if it is possible to establish some kinds of transformation relations for stellar parameters between the two databases so that they can be combined in the future study on the Galaxy. Since the APOGEE database is based on high resolution spectra with high signal-to-noise ratios, it may provide better parameters, at least for stellar metallicity, than the LAMOST database estimated from low resolution and low signal-to-noise spectra. Meanwhile, we hope to check the stellar parameters provided by the LAMOST DR2 database before they can be really used to probe the evolution of the Galaxy. Specifically, we want to know what kinds of stars in the LAMOST DR2 database have reliable parameters, and what kinds of stars show unreasonable values which should be excluded in the future Galactic study. Finally, this check and comparison might provide some clues too improve the stellar parameters in both LAMOST DR2 and APOGEE databases. In this work, we aim to select a sample of common stars with high quality spectra in both databases, compare stellar parameters and establish calibrations for individual stellar parameters if possible.

2 STAR SAMPLE AND ITS DIVISION INTO RC AND RGB SUBSAMPLES

The selection procedure of the sample stars is proceeded as follows. First, we select common stars with the same Galactic locations, (RA, DEC) within 3 arcsecs, in the LAMOST DR2 and SDSS DR12/APOGEE databases. Then we limit stars with stellar parameters in the reasonable regions of

$3000 < T_{eff} < 9000 K$, $-1.0 < \log g < 6.0$ and $-5.0 < [Fe/H] < 1.0$. Third, we select stars with high signal-to-noise spectra in both surveys, the signal-to-noise in g band of LAMOST spectra $sn_g > 30$ and the signal-to-noise of APOGEE spectra $sn > 100$. With these criteria, we have 5626 stars in common, for which the T_{eff} versus $\log g$ diagrams are shown in Fig. 1. We notice that there are some turn-off and subgiant stars. Since the APOGEE database only provides stellar parameters for giants, we thus limit our sample of stars with $\log g < 3.8$ in both database. In total, we have 5352 stars for comparison.

There are some differences in the T_{eff} versus $\log g$ diagrams between the two datasets. The most prominent difference is that the LAMOST database shows a strong clump feature in this diagram which corresponds to the well-known red clump population, which is not easily seen by eye check in the APOGEE database. The appearance of this feature proves that stellar parameters in the LAMOST database are generally reasonable at least for stars at this region. With this advantage, we select a sample of RC stars from the LAMOST database by limiting stars within the two red lines, where stars follow the relation of $-0.0010 * T_{eff,LAMOST} + 7.10 < \log g_{LAMOST} < -0.0005 * T_{eff,LAMOST} + 5.05$, and in the temperature range of $4600 < T_{eff,LAMOST} < 5000 K$. The right temperature limit of $T_{eff,LAMOST} < 5000 K$ is applied since the star number significantly decreases in the lower panel of Fig. 1, and this criterion may exclude the secondary red clump sequence, which is predicted to locate on the blue and faint-magnitude side of the main red clump sequence in the color magnitude diagram (Girardi et al. 1999). The left temperature limit of $T_{eff,LAMOST} > 4600 K$ is chosen in order to avoid the contamination of the possible bump of red giant branch at the red side of red clump at the solar metallicity. For comparison, two theoretical isochrones of 1 Gyr and 10 Gyr with $Z=0.030$ from the Padova website (<http://stev.oapd.inaf.it/cgi-bin/cmd>, Bressan et al. 2012) are overplotted in Fig. 1.

The selection procedure of RC sample is mainly based on eye check on the T_{eff} versus $\log g$ diagram of the LAMOST database. According to Bovy et al. (2014), RC stars in the APOGEE database can be selected by their position in color- metallicity-gravity-temperature space using a new method calibrated using stellar evolution models and high-quality asteroseismology data. In their Figure 1, a linear line of $\log g_{APOGEE} = 0.0018 * (T_{eff,APOGEE} - 4607) + 2.5$ at solar metallicity clearly separates RC stars from RGB stars, which is shown in red line in the upper panel of Fig. 1. When we overplot our selected RC sample of stars with green dots in the T_{eff} versus $\log g$ diagram of the APOGEE database, they locate exactly on the left edge of the red line. Thus, our RC sample generally follows the selection criteria of Bovy et al. (2014). Note that our RC sample stars do not take into account stars on the secondary red clump sequence for two reasons. First, they can be identified by seismic analysis (Stello et al. 2013) but it is difficult to pick them out from the T_{eff} versus $\log g$ diagram. Secondly, they might have different properties as compared with stars in the main RC sequence; they are massive, young and have different dependences of $\log g$ with T_{eff} . Thus, this work mainly involve with the main sequence RC stars. Finally, we divide our selected sample of 5352 stars into two samples, the RC sample with 1544 stars and the RGB sample from the remaining 3808 stars. In the following sections, the two samples will be investigated separately due to their different properties.

3 THE COMPARISON OF STELLAR PARAMETERS BETWEEN THE LAMOST AND APOGEE DATABASES

3.1 The T_{eff} , $\log g$ and $[Fe/H]$ Distributions

In order to investigate if there is any systematic shifts in stellar parameters between the LAMOST and APOGEE databases, we show the distributions of T_{eff} , $\log g$ and $[Fe/H]$ in Fig. 2 for the whole sample. It shows that there are systematic shifts in the $\log g$ and $[Fe/H]$ distributions but not clear difference for the T_{eff} distribution between the two datasets. For gravity, the LAMOST dataset shows one peak at $\log g \sim 2.3 - 2.4$, while the APOGEE dataset has the main peak at $\log g \sim 2.5 - 2.6$ and possible second peak at $\log g \sim 2.85$, which may correspond to the secondary red clump sequence according to Bovy et al. (2014). For metallicity, there is a prominent shift in the metallicity peak from $[Fe/H] \sim -0.1$ in the APOGEE dataset to $[Fe/H] \sim -0.3$ in the LAMOST dataset as well as the whole shift of the

distributions at the metal rich side. In addition, most stars have metallicity in the range of $-1.0 < [\text{Fe}/\text{H}] < 0.5$ indicating the dominate population of the Galactic disk in our sample. Note that the adopted $\log g$ and $[\text{Fe}/\text{H}]$ values in the APOGEE database have been corrected by equations (3) and (6) of [Holtzman et al. \(2015\)](#), without which the differences between the two datasets will be even larger.

Fig. 3 shows the $[\text{Fe}/\text{H}]$ and $\log g$ distributions for RC and RGB samples, respectively. Clearly, the metallicity shift is systematic, and RC and RGB samples behave in a similar way. The systematic shift of gravity in Fig. 2 mainly comes from the RC sample, and it is not so prominent for RGB sample. Instead, the APOGEE dataset shows a slightly broader $\log g$ distribution than the LAMOST dataset. Moreover, as shown in Fig. 1, the dependence of $\log g$ with T_{eff} in the RC sample is opposite between the LAMOST and APOGEE dataset. In view of these different properties for RC and RGB samples, it is reasonable to establish the calibrations for RC and RGB stars separately.

3.2 The Comparison and Calibrations of Stellar Parameters

If possible, we aim to establish the calibrations of stellar parameters between the LAMOST and APOGEE datasets in order to combine the two surveys in the future study. For this purpose, the one-to-one comparisons of T_{eff} , $\log g$ and $[\text{Fe}/\text{H}]$ for RC (left panels) and RGB (right panels) samples between the LAMOST and APOGEE databases are shown in Fig. 4. Stars with $[\text{Fe}/\text{H}] < -1$ are marked by red crosses since they only contribute small parts of our main population of the Galactic disk with $[\text{Fe}/\text{H}] > -1$ (see Fig. 2).

Note that most stars in our RC sample have $[\text{Fe}/\text{H}] > -0.8$ which is consistent with the metallicity distribution of local RC stars as shown in [Puzeras et al. \(2010\)](#). However, 22 stars in our RC sample have $[\text{Fe}/\text{H}] < -1$, which is outside the metallicity range of local RC sample of $-0.8 < [\text{Fe}/\text{H}] < 0.3$ (their Figure 5). We marked these RC stars with $[\text{Fe}/\text{H}] < -1$ by red crosses in the left panels of Fig. 4. We find that they do not follow the general trends of most RC stars in both T_{eff} and $\log g$ panels of Fig. 4. Thus, they might not be real RC stars. Instead, they could be red horizontal branch or metal poor red giant stars, but it is difficult for us to distinguish them. Thus, these stars are excluded in the following analyses. For RC stars, the agreement in T_{eff} between the LAMOST and APOGEE datasets is good with a std scatter of 53 K around the calibration of $T_{\text{eff,APOGEE}} = 0.95 * [\text{Fe}/\text{H}]_{\text{LAMOST}} + 210$. Note that significant deviations in the temperature comparison from the one-to-one line at both ends mainly come from the selection criterion of $4600 < T_{\text{eff,LAMOST}} < 5000$ K for RC stars. However, there is no any correlation or any kind of anti-correlation in the $\log g$ comparison, and the scatters are too large to obtain reliable calibrations. For metallicity, a good calibration of $[\text{Fe}/\text{H}]_{\text{APOGEE}} = 1.16 * [\text{Fe}/\text{H}]_{\text{LAMOST}} + 0.14$ with a scatter of 0.065 dex can be established for RC stars with $[\text{Fe}/\text{H}] > -1$.

For RGB stars, a similar metallicity calibration of $[\text{Fe}/\text{H}]_{\text{APOGEE}} = 1.18 * [\text{Fe}/\text{H}]_{\text{LAMOST}} + 0.11$ ($\sigma = 0.08$) as RC sample is found, and we may establish a T_{eff} calibration of $T_{\text{eff,APOGEE}} = 0.86 * T_{\text{eff,LAMOST}} + 665$ with a scatter of 77 K. For gravity, the general trend in the comparison follows the one-to-one line, but there are very large scatters in the range of $1.5 < \log g_{\text{LAMOST}} < 2.6$. Moreover, stars with $[\text{Fe}/\text{H}] < -1$, marked by red crosses again, have systematically higher value by ~ 0.2 dex for stars with $\log g_{\text{LAMOST}} > 1.0$. In view of this difference, we establish two gravity calibrations for RGB stars with a metallicity division at $[\text{Fe}/\text{H}] = -1$, $\log g_{\text{APOGEE}} = 0.92 * \log g_{\text{LAMOST}} + 0.09$ for $[\text{Fe}/\text{H}] > -1$ and $\log g_{\text{APOGEE}} = 0.90 * \log g_{\text{LAMOST}} + 0.34$ for $[\text{Fe}/\text{H}] < -1$, with a scatter of 0.24 in both calibrations. When the temperature term is included, the scatters are slightly reduced with calibrations of $\log g_{\text{APOGEE}} = 0.00105 * T_{\text{eff,LAMOST}} + 0.46 * \log g_{\text{LAMOST}} - 3.85$ ($\sigma = 0.20$) for $[\text{Fe}/\text{H}] < -1$ and of $\log g_{\text{APOGEE}} = 0.00087 * T_{\text{eff,LAMOST}} + 0.59 * \log g_{\text{LAMOST}} - 3.11$ ($\sigma = 0.17$) for $[\text{Fe}/\text{H}] > -1$. As we further include the metallicity term, the calibrations are of $\log g_{\text{APOGEE}} = 0.00140 * T_{\text{eff,LAMOST}} + 0.28 * \log g_{\text{LAMOST}} + 0.20 * [\text{Fe}/\text{H}]_{\text{LAMOST}} - 4.89$ ($\sigma = 0.20$) for $[\text{Fe}/\text{H}] < -1$ and of $\log g_{\text{APOGEE}} = 0.00107 * T_{\text{eff,LAMOST}} + 0.46 * \log g_{\text{LAMOST}} + 0.34 * [\text{Fe}/\text{H}]_{\text{LAMOST}} - 3.64$ ($\sigma = 0.15$) for $[\text{Fe}/\text{H}] > -1$.

3.3 Refine the $\log g$ calibrations for RGB stars with $[\text{Fe}/\text{H}] > -1$

In order to probe the large scatter in the $\log g$ calibration between the APOGEE and the LAMOST datasets for RGB stars, we carefully inspect their differences in the T_{eff} versus $\log g$ diagrams in Fig. 5. It shows that the main discrepancy comes from the lack of stars on the right side of the blue dash line, which can be expressed by the relation of $\log g = 0.00253 * T_{\text{eff}} - 8.67$ by passing the two points in $(T_{\text{eff}}, \log g)$ of (3500, 0.2) and (5000, 4.0). The solid line in the left-upper panel of Fig. 5 shows an extreme case with an isochrone of 16 Gyr at the metallicity of $Z = 0.030$ from Padova group (Bressan et al. 2012), and we find substantial number of stars in the LAMOST dataset locate on the right side of this extreme case. We thus define a forbidden region where no theoretical model could predict such kind of stellar parameters. Taking into account of temperature and gravity uncertainties as well as the theoretical isochrone of 16 Gyr at $Z = 0.030$, we may assign stars with $\log g_{\text{LAMOST}} < 2.6$ in the LAMOST dataset and locating on the right side of blue line belonging to a forbidden region; they are marked by blue dots in all panels of Fig. 5. Obviously, these blue dots locate below the one-to-one line in the comparison of $\log g$ in the left-lower panel of Fig. 5, indicating the LAMOST values are too high as compared with the APOGEE values. These stars become one of the main sources of the $\log g$ scatter in the comparison, and thus they should be excluded in the calibrations.

Meanwhile, recall that our selection criteria of RC stars are quite strict in order to obtain a clear sample, and thus our RGB sample from the remaining stars is somewhat contaminated by some RC stars. In particular, the secondary RC stars if existed, locate at the blue side of the main RC sequence, are included in our RGB sample. We notice that these stars can be distinguished by matching their locations in the T_{eff} versus $\log g$ diagram with their metallicities in the sense that metal poor RGB stars with $[\text{Fe}/\text{H}] < -1$ will locate at the blue side of the green dash line, which arbitrarily shift the blue line by 400 K in temperature. We do not adopt the theoretical isochrone of 16 Gyr at the metallicity of $Z = 0.030$ from Padova group (Bressan et al. 2012) because they do not fit the LAMOST dataset statistically. But we have checked that the shift of 400 K in temperature corresponds to the change of RGB ridge lines from solar metallicity to $[\text{Fe}/\text{H}] = -1$. Specifically, stars with $[\text{Fe}/\text{H}] > -1$ but locating on the blue side of the green dash line could be RC stars instead of RGB stars or RGB stars with wrong stellar parameters. These stars are marked by green dots in Fig. 5, and they constitute the second main source of scatter in the $\log g$ comparison. Generally, they have higher $\log g$ values in the APOGEE dataset than those of the LAMOST databases. These stars are further excluded in the calibration.

After excluding stars from the above two regions, we repeat the procedures and obtain the calibration of $\log g_{\text{APOGEE}} = 0.000615 * T_{\text{eff,LAMOST}} + 0.697 * \log g_{\text{LAMOST}} - 2.208$ ($\sigma = 0.150$) for RGB stars with $[\text{Fe}/\text{H}] > -1$. The same procedures are performed from the APOGEE dataset to the LAMOST dataset, and we obtain the calibration of $\log g_{\text{LAMOST}} = -0.000941 * T_{\text{eff,APOGEE}} + 1.344 * \log g_{\text{APOGEE}} + 3.674$ ($\sigma = 0.167$) for $[\text{Fe}/\text{H}] > -1$.

3.4 On the Gravity Discrepancy of RC stars

As described in Holtzman et al. (2015), RC stars in the APOGEE database are calibrated as the same equation (Eq. 3) as RGB stars. This is not the best solution for RC stars. Instead, the comparison of $\log g$ between the raw ASPCAP values (Garcia et al. 2015) and the seismic ones from the APOKASC catalog (Pinsonneault et al. 2014) in the Kepler field indicates a difference of 0.15 dex between RC and RGB stars (Holtzman et al. 2015). That means we need to reduce $\log g$ in the APOGEE database by a further order of 0.15 dex for RC stars. If this difference is applied, the $\log g$ distributions between the LAMOST and APOGEE databases in the left-lower panel of Fig. 3 are consistent. This consistency shows that the LAMOST $\log g$ for RC stars is on the same scale as that of the seismic values from the Kepler survey.

The second discrepancy for RC stars between the LAMOST and the APOGEE databases (see Fig. 1) is the opposite dependence of $\log g$ on T_{eff} . In the LAMOST dataset, $\log g$ increases with decreasing T_{eff} with a slope of -0.68 dex per 1000 K, while the slope is of 0.89 dex per 1000 K in the APOGEE dataset. This discrepancy is the same as we limit stars with $[\text{Fe}/\text{H}] > -0.5$ in both samples. Since the selection of RC stars is carried out in the LAMOST dataset and we limit stars in the LAMOST

temperature range of $4600 < T_{eff} < 5000$ K, the slope of -0.68 dex per 1000 K just reflects our selection criteria of $-0.0010 * T_{eff,LAMOST} + 7.10 < logg_{LAMOST} < -0.0005 * T_{eff,LAMOST} + 5.05$. Moreover, the slope will be reduced after excluding a few stars at $T_{eff} \sim 4980$ K and $logg \sim 2.1$, and the scatter of 0.10 dex at a given T_{eff} will significantly affect this slope. However, there is a strong dependence of $logg$ on T_{eff} in the APOGEE database, which can not be explained by its scatter. The strong dependence of $logg$ on T_{eff} persists even the systematic shift of 0.15 dex is applied to RC stars in the APOGEE database.

Since our sample of RC stars fits well the selection criteria of Bovy et al. (2014), we can expect that they are real RC stars in both databases. With this agreement, we plot an independent sample of RC stars from Casagrande et al. (2014) by red open circle in Fig. 6 and compare the dependence trends of $logg$ on T_{eff} among the three datasets. Note that the RC sample in Casagrande et al. (2014) has several advantages. (i) RC stars are identified by seismic data with period space from Stello et al. (2013) and they have accurate seismic $logg$. (ii) They have strömgren $(b - y)_0$ colors, which are very sensitive to temperature. (iii) Casagrande et al. (2014) provide mass and age for RC stars, which allow us to limit stars with $mass < 1.8M_{\odot}$ and $age > 2$ Gyr in order to exclude the RC stars on the secondary sequence. Clearly, there is no slope in the T_{eff} versus $logg$ diagram, and most stars have $logg = 2.4 - 2.6$. The LAMOST data agree with Casagrande et al. (2014) for RC stars in a better way than the APOGEE database. Careful inspection of the Figure 4 of Holtzman et al. (2015), there is a hint of increasing trend of $\Delta logg(ASPCAP - Kelper)$ with increasing $logg_{ASPCAP}$ for RC stars (blue squares). If this trend is applied to the APOGEE database, the slope in the T_{eff} versus $logg$ diagram for RC stars in the APOGEE databases will be slightly reduced. But further work on this correction should be done in the future.

3.5 New LAMOST Gravities from SVM with Seismic Basement

As described above, the LAMOST database do not provide the best gravities for giant stars in the forbidden region and the slope in the T_{eff} versus $logg$ diagram for RC stars is not consistent with that from the SAGA survey by Casagrande et al. (2014). Is there some way to improve these gravities? Recently, Liu et al. (2015) present a support vector machine (hereafter SVM) method to derive gravities for LAMOST giants based on a sample of stars with seismic $logg$ in Huber et al. (2014) as a training dataset. In this training dataset, $logg$ values in Huber et al. (2014) has been re-calculated with the LAMOST T_{eff} , and thus these new gravities in Liu et al. (2015) match T_{eff} values in the LAMOST database used in the present work.

It is interesting to investigate how stars in the forbidden and unmatched regions in Fig. 5 behave with these new gravities. Fig. 7 shows the T_{eff} versus $logg_{SVM}$ diagram for 4915 stars. Interestingly, most stars in the forbidden region (blue dots) locate around the blue dash line, on the right side of which the APOGEE database is lack of stars. Clearly, new gravities from Liu et al. (2015) seem to be more reasonable and they are consistent with those in the APOGEE database in this region within the errors. Meanwhile, a substantial number of stars in the unmatched region in Fig. 5 locate at the left part of the main RC stars, indicating that they are probably also main RC stars instead of secondary ones. In addition, the main feature of RC stars becomes quite prominent in the T_{eff} versus $logg_{SVM}$ diagram as stars in the unmatched region of in Fig. 5 are included. However, the selection of stars within the two red lines may not be suitable based on new gravities. Instead, there is not significant dependence of $logg$ with T_{eff} for the main RC feature. In Fig. 8, we plot the T_{eff} versus $logg_{SVM}$ diagram for our selected RC sample of stars with $[Fe/H] > -0.5$. The slope is of 0.18 dex per 1000 K which is consistent with that from the SAGA survey by Casagrande et al. (2014).

4 SUMMARY

We have compared the stellar parameters, T_{eff} , $logg$ and $[Fe/H]$, between the LAMOST and the APOGEE datasets. We have identified the main sequence of RC stars in the T_{eff} versus $logg$ diagram of the LAMOST dataset, which behaves in a more reasonable way than that in the APOGEE datasets.

For RGB stars, the LAMOST dataset spans a wider range than the APOGEE dataset in the T_{eff} versus $\log g$ diagram, and a group of stars with $2.6 > \log g > 0.00253 * T_{eff} - 8.67$ locates at a forbidden region where no theoretical model predicts such kinds of stellar parameters. We further exclude stars with their metallicity of $[Fe/H] > -1$ unmatched with their positions in the T_{eff} versus $\log g$ diagram (outside the green dash line where RGB stars with $[Fe/H] < -1$ locate).

We have established a good metallicity calibration of $[Fe/H]_{APOGEE} = 1.18 * [Fe/H]_{LAMOST} + 0.11$ ($\sigma = 0.08$) for both RC and RGB stars, and a temperature calibration of $T_{eff_{APOGEE}} = 0.95 * T_{eff_{LAMOST}} + 210$ ($\sigma = 53 K$) in consistent with the one-to-one line within the measured errors. There is no clear trend in gravity between the LAMOST and the APOGEE datasets for RC stars, and we may prefer the the LAMOST dataset rather than the APOGEE dataset since the former follows the general trend of increasing $\log g$ with decreasing T_{eff} , which is the RC feature as seen in the CMD of local RC stars in the field and some old open clusters. For example, the CMD of an old open cluster NGC6819 in Lee-Brown et al. (2015) shows that V magnitude becomes fainter (corresponding to the decrease of luminosity) as $(B - V)$ color goes redder (indicating the decreasing temperature). However, the RC sample of Casagrande et al. (2014) do not show this dependence, and we need further study to clarify if the dependence of $\log g$ with T_{eff} for RC stars is true. For RGB stars, we prefer calibrations of $\log g_{APOGEE} = 0.000874 * T_{eff_{LAMOST}} + 0.588 * \log g_{LAMOST} - 3.117$ ($\sigma = 0.167$) for $[Fe/H] < -1$ and $\log g_{APOGEE} = 0.000615 * T_{eff_{LAMOST}} + 0.697 * \log g_{LAMOST} - 2.208$ ($\sigma = 0.150$) for $[Fe/H] > -1$ after excluding stars in the forbidden region and the unmatched region of the T_{eff} versus $\log g$ diagram. Finally, we have found that new gravities from the SVM method based on the seismic $\log g$ by Liu et al. (2015) are more reliable than the original values in the LAMOST database for stars in both the forbidden and the unmatched regions.

Acknowledgements This study is supported by the National Natural Science Foundation of China under grant Nos. 11222326, 11233004, 11390371, the Strategic Priority Research Program of the Chinese Academy of Sciences Grant No. XDB01020300 and the National Key Basic Research Program of China (973 program) Nos. 2014CB845701/703.

Guoshoujing Telescope (the Large Sky Area Multi-Object Fiber Spectroscopic Telescope LAMOST) is a National Major Scientific Project built by the Chinese Academy of Sciences. Funding for the project has been provided by the National Development and Reform Commission. LAMOST is operated and managed by the National Astronomical Observatories, Chinese Academy of Sciences.

Funding for SDSS-III has been provided by the Alfred P. Sloan Foundation, the Participating Institutions, the National Science Foundation, and the U.S. Department of Energy Office of Science. The SDSS-III web site is <http://www.sdss3.org/>. SDSS-III is managed by the Astrophysical Research Consortium for the Participating Institutions of the SDSS-III Collaboration including the University of Arizona, the Brazilian Participation Group, Brookhaven National Laboratory, University of Cambridge, University of Florida, the French Participation Group, the German Participation Group, the Instituto de Astrofísica de Canarias, the Michigan State/Notre Dame/JINA Participation Group, Johns Hopkins University, Lawrence Berkeley National Laboratory, Max Planck Institute for Astrophysics, New Mexico State University, New York University, Ohio State University, Pennsylvania State University, University of Portsmouth, Princeton University, the Spanish Participation Group, University of Tokyo, University of Utah, Vanderbilt University, University of Virginia, University of Washington, and Yale University.

References

- Ahn C., Alexandroff R., Allende Prieto C., et al. 2012, ApJS, 203, 21
- Bovy, J., Nidever, D. L., Rix, H.-W., et al. 2014, ApJ, 790, 127 [3](#), [6](#)
- Bressan A., Marigo P., Girardi L., Salasnich B., Dal Cero C., Rubele S., Nanni A. 2012, MNRAS, 427, 127
- Casagrande, L., Silva Aguirre, V., Stello, D., et al. 2014, ApJ, 787, 110 [6](#), [14](#), [16](#)
- De Cat, P; Fu, J.N. et al. 2014, submitted

- Cui X.Q., Zhao Y.H., Chu Y.Q., et al., 2012, RAA, 12, 9, 1197
- Eisenstein D.J., Weinberg D.H., Agol E., et al. 2011, AJ 142, 72
- García Pérez, A. E., Allende-Prieto, C., Holtzman, J., et al. 2015, in preparation
- Girardi L., 1999, MNRAS, 308, 818
- Holtzman, J. A., Shetrone, M., Johnson, J. A. 2015, arXiv, 1501.04110
- Huber, D., Silva Aguirre, V., Matthews, J. M., et al. 2014, ApJS, 211, 2
- Lee-Brown D.B., Anthony-Twarog B.J., Deliyannis, C.P., Rich, E., Twarog B.A. 2015, AJ, 149, 121 [4](#), [5](#), [6](#)
- Liu, C. et al., 2015, ApJ, submitted [6](#)
- Luo A.L., Bai Z.R. et al. 2015, RAA, in press [7](#)
- Kordopatis G. et al., 2013, AJ, 146, 134 [6](#), [7](#), [15](#), [16](#)
- Majewski, S. R., Schiavon, R. P., Allende Prieto, C., et al. 2015, in preparation
- Puzeras E., Tautvaišienė G., Cohen J.G., Gray D.F., Adelman S.J., Ilyin I., Chorniya Y., 2010, MNRAS, 408, 1225
- Pinsonneault, M. H., Elsworth, Y., Epstein, C., et al. 2014, ApJS, 215, 19
- Stello, D., Huber, D., Bedding, T. R., et al. 2013, ApJ, 765, L41 [4](#)
- Wu, Y., Luo, A-L., Li, H-N. et al., 2011, RAA, 11, 924
- Yanny B., Rockosi C., Newberg H.J., et al. 2009, AJ, 137, 4377 [6](#)
- Zhao, G., Zhao, Y.H., Chu, Y.Q., et al. 2012, RAA, 12, 723

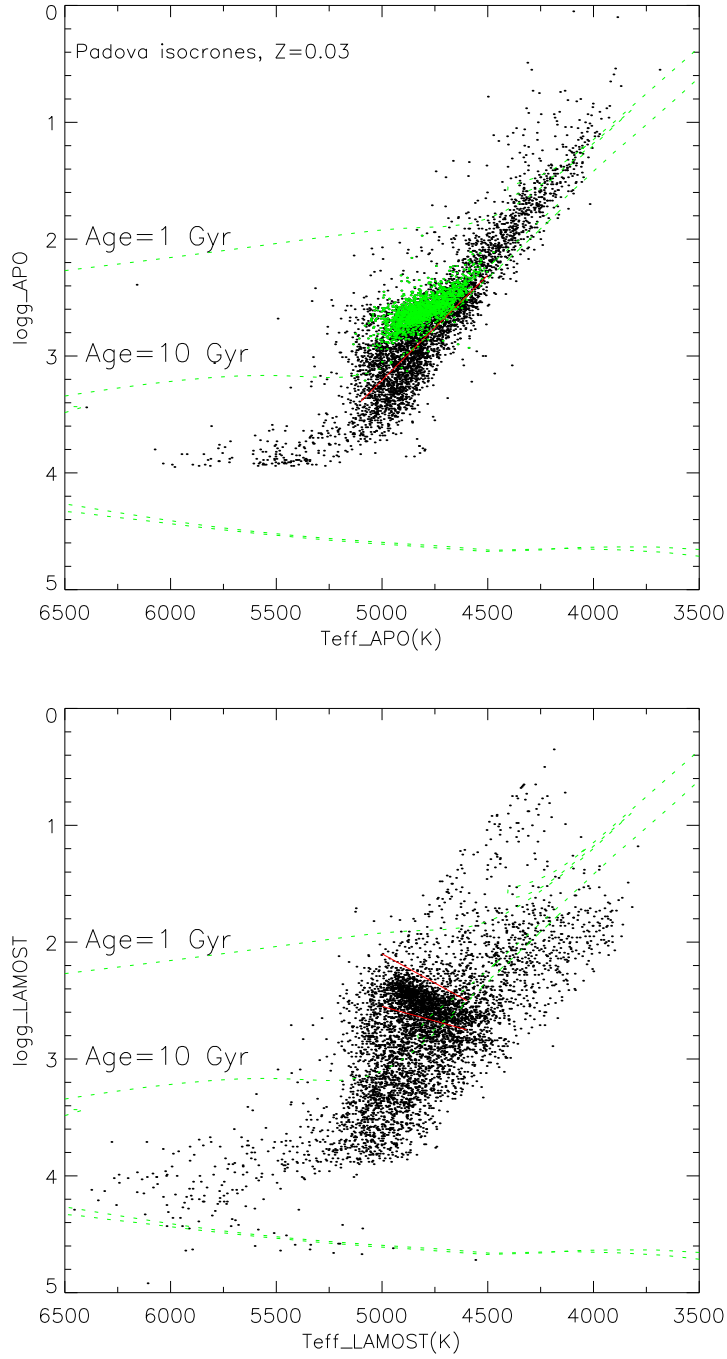


Fig. 1 The T_{eff} versus $\log g$ diagrams for the LAMOST (lower panel) and APOGEE (upper panel) databases based on 5626 common stars with high quality spectra (LAMOST: $sng > 30$, APOGEE: $sn > 100$). Dashed lines show theoretical isochrones of 1 and 10 Gyr at $Z=0.030$ from the Padova website (Bressan et al. 2012). The selection criteria of RC stars are marked in red lines, and green dots in the upper panel are our sample of RC stars selected from the LAMOST database.

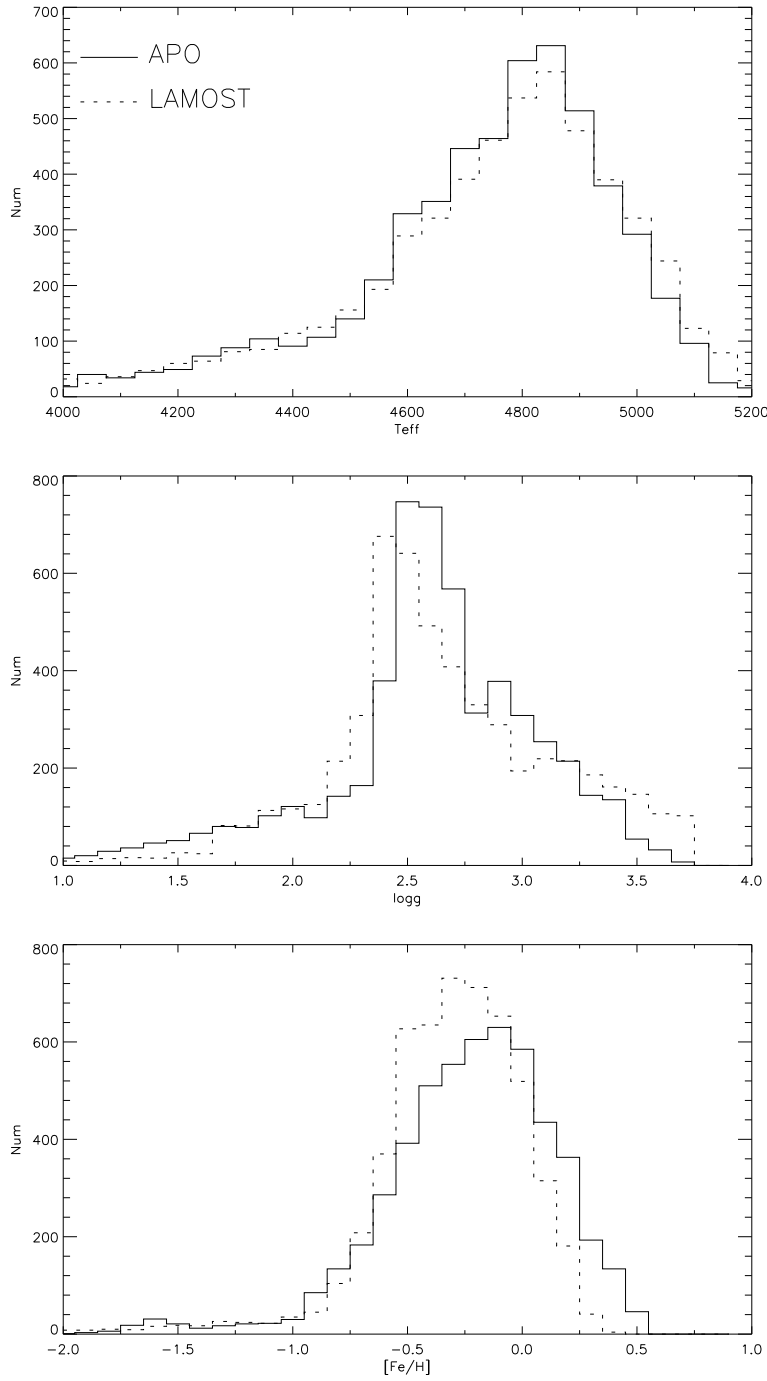


Fig. 2 The distributions of T_{eff} , $\log g$ and $[Fe/H]$ for the whole sample based on the LAMOST (dash lines) and APOGEE (solid lines) databases.

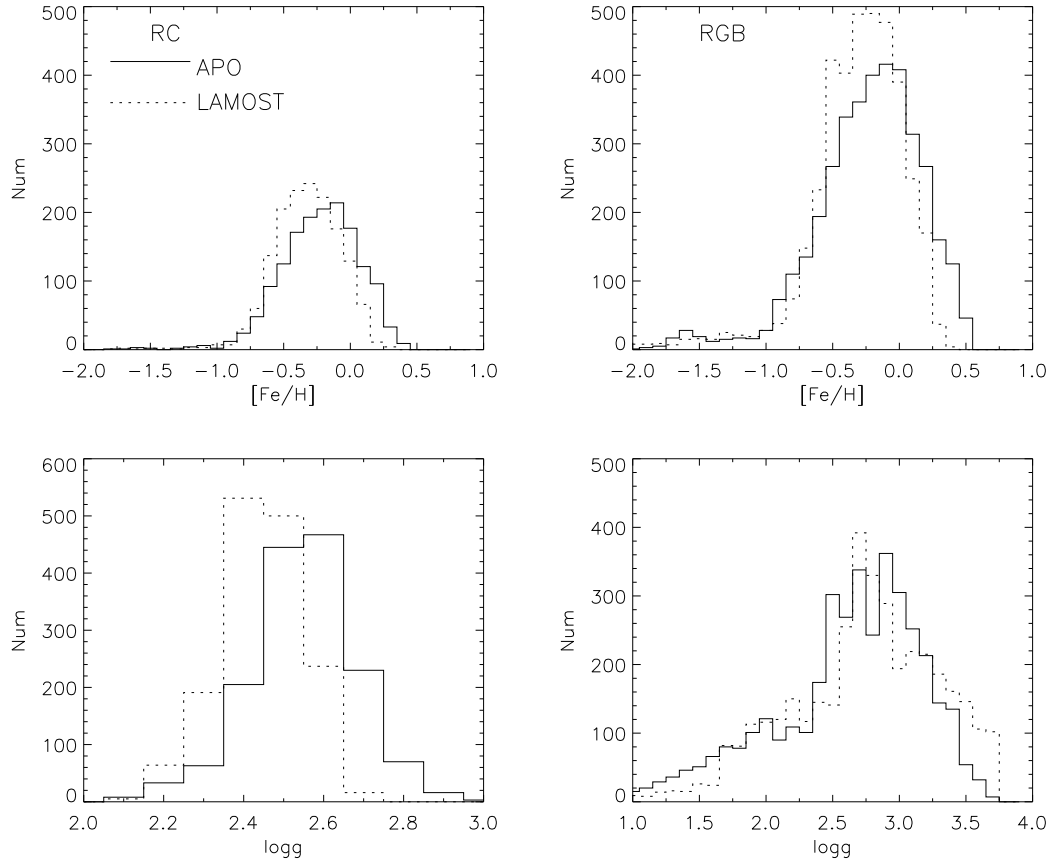


Fig. 3 The distributions of $\log g$ and $[\text{Fe}/\text{H}]$ for RC (left) and RGB (right) stars based on the LAMOST (dash lines) and APOGEE (solid lines) databases.

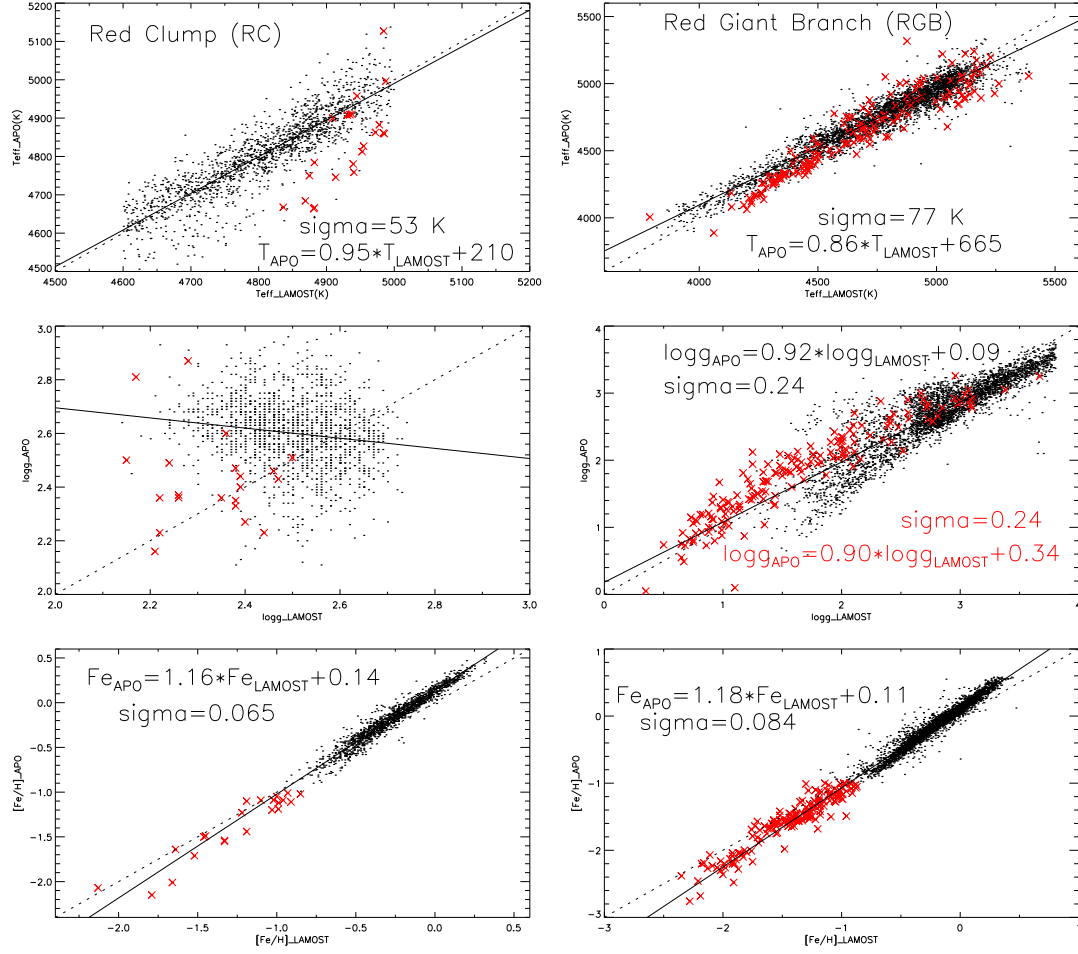


Fig. 4 The comparisons and calibrations of T_{eff} , $\log g$ and $[Fe/H]$ between the LAMOST and APOGEE databases for RC (left panels) and RGB (right panels) samples. Dashed lines are the one-to-one relations while solid lines are the calibrations. Stars with $[Fe/H] < -1$ are indicated by red crosses.

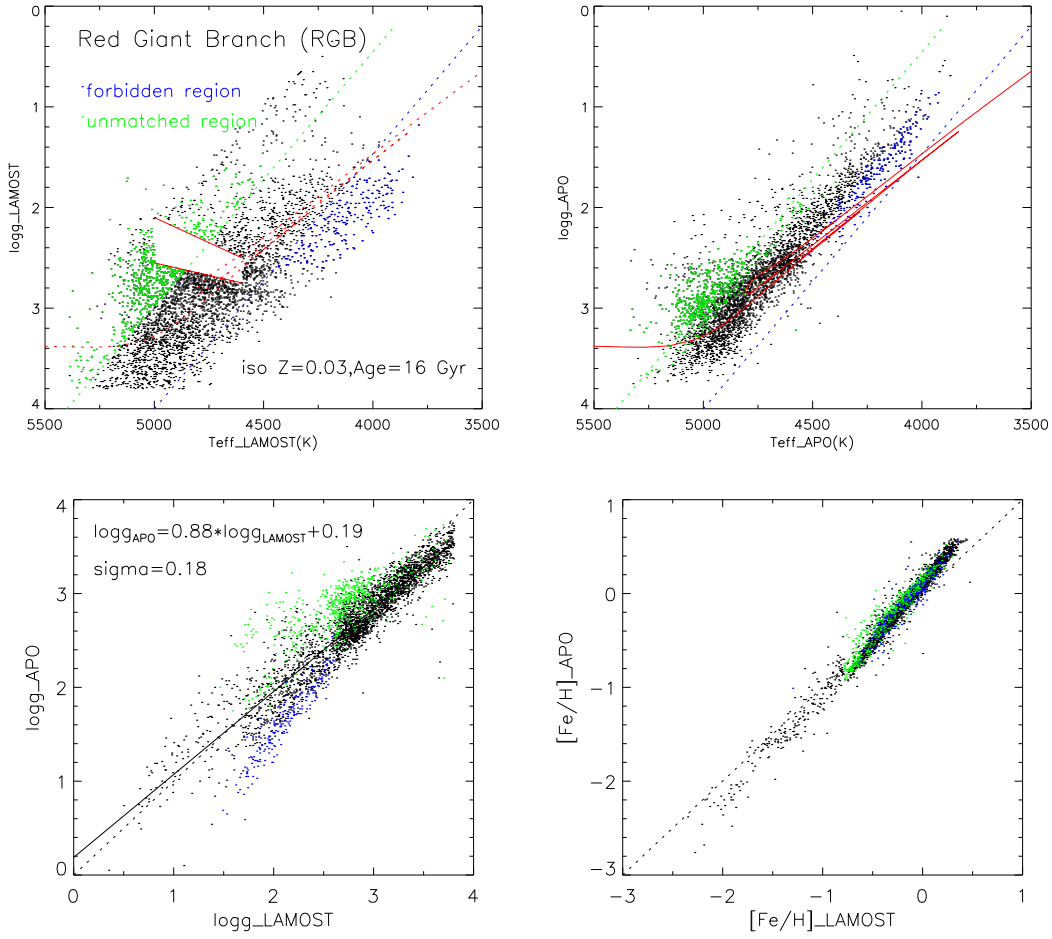


Fig. 5 Upper: The T_{eff} versus $\log g$ diagrams for RGB stars in the LAMOST and APOGEE datasets. Blue dash line is passing two points at $(T_{\text{eff}}, \log g)$ of (3500, 0.2) and (5000, 4.0) and red dash line is the sochrone of 16 Gyr at $Z = 0.030$ from Padova group (Bressan et al. 2012). Lower: The comparison of gravity and metallicity for different groups of RGB stars. Stars with $2.6 > \log g > 0.00253 \cdot T_{\text{eff}} - 8.67$ at the forbidden region are marked by blue dots and stars at the unmatched region are marked by green dots.

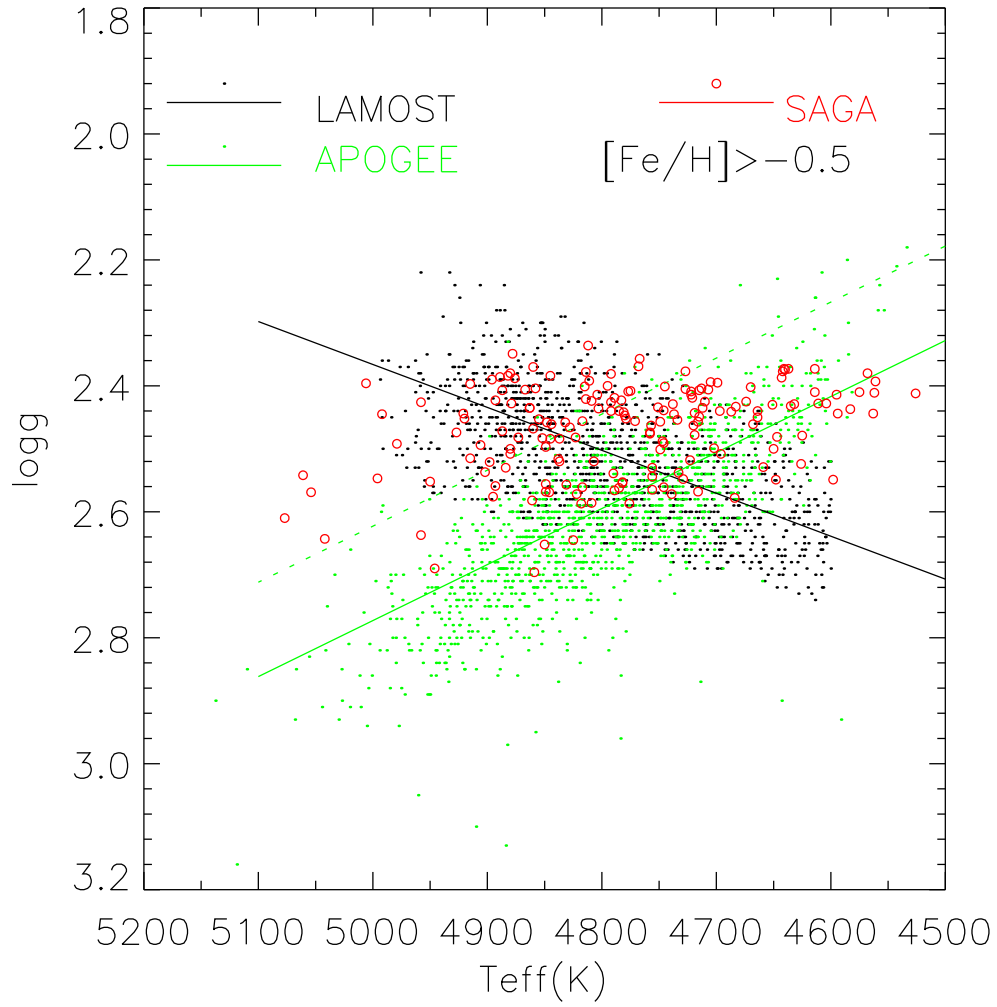


Fig. 6 The comparison of the T_{eff} versus $\log g$ diagram for RC stars in the LAMOST and APOGEE datasets with that from the SAGA survey by [Casagrande et al. \(2014\)](#).

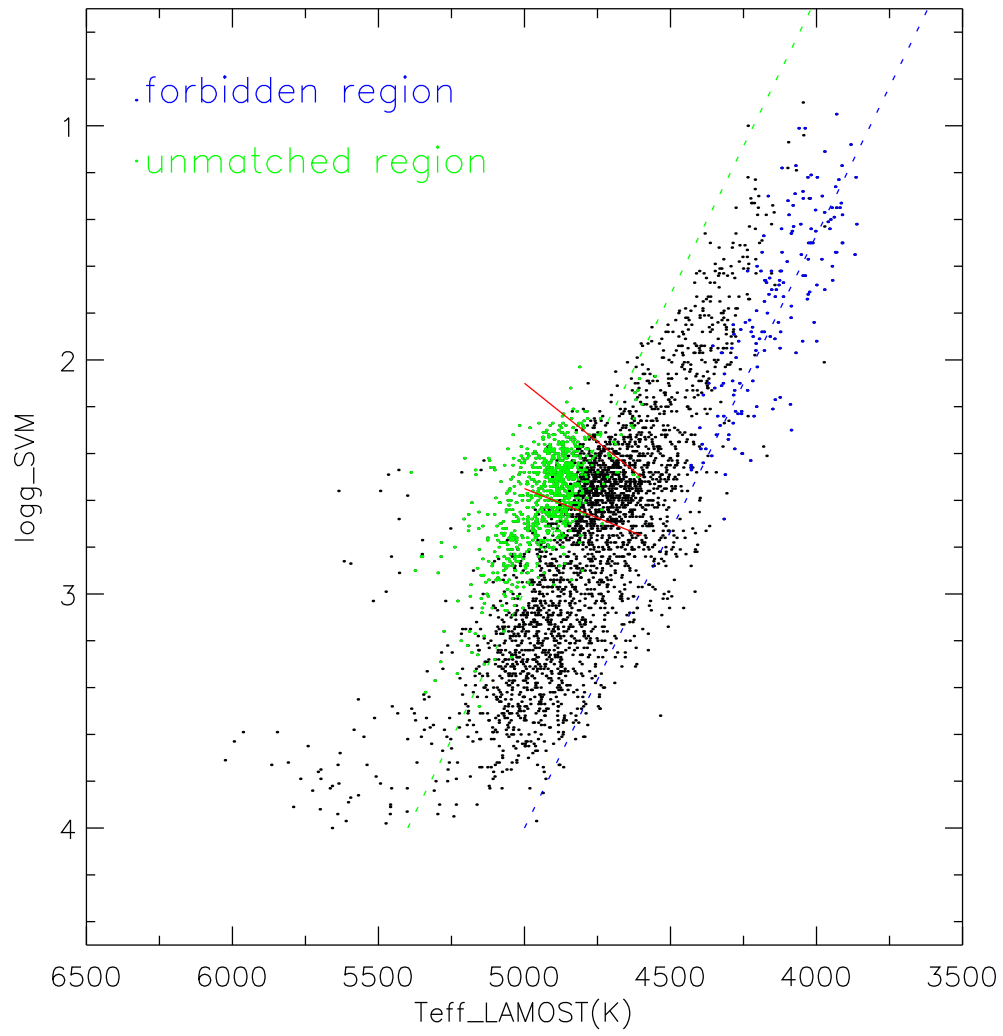


Fig. 7 The comparison of the T_{eff} versus $\log g$ diagram based on new gravities from [Liu et al. \(2015\)](#). The symbols are the same as in the left-upper panel of Fig. 4.

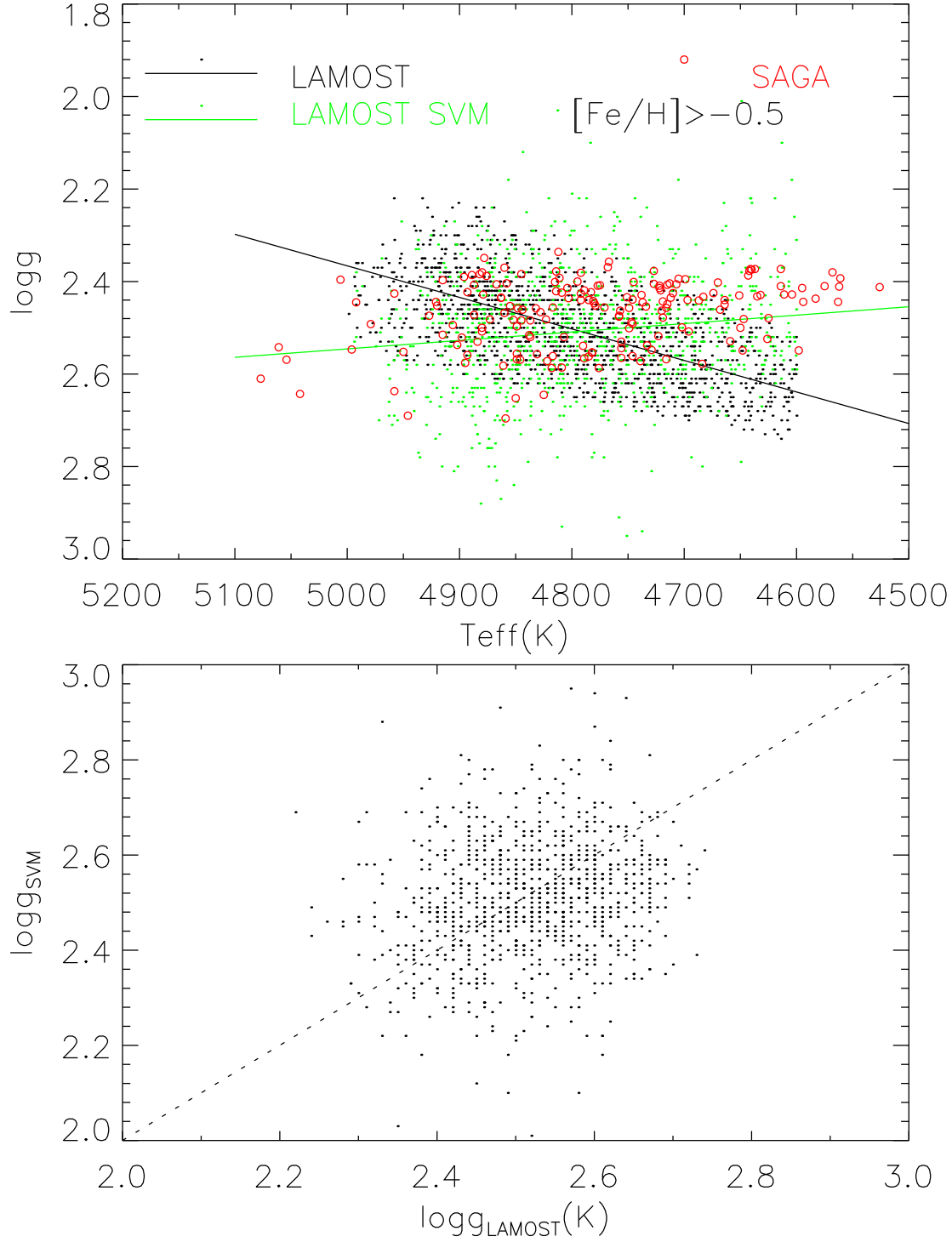


Fig. 8 The slope comparison in the T_{eff} versus $\log g$ diagram for RC stars among new gravities from [Liu et al. \(2015\)](#), the LAMOST dataset and the SAGA survey by [Casagrande et al. \(2014\)](#).